© Pol J Radiol 2022; 87: e316-e324
DOI: https://doi.org/10.5114/pjr.2022.117590

Received: 30.05.2021
Accepted: 15.08.2021
Published: 13.06.2022

Polish Journal of Radiology

http://www.polradiol.com

Original paper

Interrater reliability and agreement of the liver imaging reporting and data system (LI-RADS) v2018 for the evaluation of hepatic lesions

Ahmed S. Abdelrahman[A,B,C,E,F], Sherihan S. Madkour[B,D,F], Mena E.Y. Ekladious[B,D,E,F]

Department of Radiology, Faculty of Medicine, Ain Shams University, Cairo, Egypt

Abstract

Purpose: The liver imaging reporting and data system (LI-RADS) is a structured reporting system that categorizes hepatic observations according to major imaging features and lesion size, with an optional ancillary features contribution. This study aimed to evaluate inter-reader agreement of dynamic magnetic resonance imaging (MRI) using LI-RADS v2018 lexicon.

Material and methods: Forty-nine patients with 69 hepatic observations were included in our study. The major and ancillary features of each hepatic observation were evaluated by 2 radiologists using LI-RADS v2018, and the inter-reader agreement was allocated.

Results: The inter-reader agreement of major LI-RADS features was substantial; κ of non-rim arterial hyperenhancement, non-peripheral washout appearance, and enhancing capsule was 0.796, 0.799, and 0.772 ($p < 0.001$), respectively. The agreement of the final LI-RADS category was substantial with $\kappa = 0.651$ ($p < 0.001$), and weighted $\kappa = 0.786$ ($p < 0.001$). The inter-reader agreement of the ancillary features was substantial to almost perfect (κ range from 0.718 to 1; $p < 0.001$). An almost perfect correlation was noted for the hepatic lesion size measurement with ICC = 0.977 ($p < 0.001$).

Conclusions: The major and ancillary features of the LI-RADS v2018, as well as the final category and lesions size, have substantial to almost perfect inter-reader agreement.

Key words: LI-RADS, HCC, MRI, APHE.

Introduction

Hepatocellular carcinoma (HCC) is the most common primary malignancy of the liver, the sixth most common carcinoma in the world, and the fourth most common cause of cancer mortality [1,2]. HCC usually occurs in viral and non-viral cirrhotic liver. Hepatitis B and C viruses account for about 80% of HCC worldwide [3]. The diagnosis of HCC is based on typical imaging features in high-risk patients because lesion biopsy has several complications including haemorrhage, inadequate sampling, and seeding along the biopsy tract; thus, there is an increased need for fixed reproducible terms to standardize patient management [4].

Structured reporting with standardization of the radiological finding serves to increase the diagnostic accuracy of the report [5]. It also reduces the reporting variability and gives a definite answer for the clinician's question. The American College of Radiology (ACR) has developed and updated the liver imaging reporting and data system (LI-RADS); a standardized structured reporting system for interpreting the imaging features of the hepatic focal lesion by different contrast-enhancing imaging modalities.

The LI-RADS lexicon imaging features are divided into major criteria encompassed of non-rim arterial hyperenhancement (APHE), non-peripheral washout appearance (washout), and capsular enhancement and an optional

Correspondence address:
Ahmed S. Abdelrahman, Department of Radiology, Faculty of Medicine, Ain Shams University, Cairo, Egypt, e-mail: dr_ahmedsamy@yahoo.com

Authors' contribution:
A Study design · **B** Data collection · **C** Statistical analysis · **D** Data interpretation · **E** Manuscript preparation · **F** Literature search · **G** Funds collection

ancillary feature; combinations of both major and ancillary features with lesion size and threshold growth are intrinsic steps for defining the LI-RADS category [6]. The goal of the LI-RADS scoring system is to establish a consistent terminology that facilitates the communication with clinicians, reducing misinterpretation, allowing definitive diagnosis of the hepatic focal lesion that fulfils the criteria of HCC, and risk stratification of other hepatic lesions that do not fulfil the HCC imaging criteria [7,8]. Although LI-RADS was first published several years ago, it has since undergone many improvements. The standardized reports should be a dynamic framework that will be refined and changed as new information and data are accumulated. More research is required to recognize whether the updated LI-RADS v2018 has enhanced inter-reader agreement.

The aim of the study was to assess the reliability and the inter-observer agreement of the major features of LI-RADS v2018 using dynamic magnetic resonance imaging (MRI) and to evaluate the reducibility of ancillary features and hepatic lesion size.

Material and methods

Patients

This study was conducted in our institution after the approval of our ethical committee and informed consent was waived. Adult (over the age of 18 years) patients with risk of developing HCC including patient with cirrhosis, chronic hepatitis B, or HCC were included. Contrast-enhanced dynamic MRI examination was performed for all patients in the period between August 2020 and March 2021. Ten patients were omitted from the study because they had HCC that was treated by local-regional treatment with no new observation in the dynamic MRI study, 5 patients because of motion artifact and low-quality scan, and 3 patients because a non-contrast MRI study was conducted. Finally, the study included 49 patients (35 males and 14 females), ranging in age from 29 to 82 years old.

Technique of dynamic magnetic resonance imaging examination

The MRI examination was done using a 1.5 T MRI (Philips Achieva scanner, Healthcare, Netherlands) with a body coil. FOV: 333 × 273 × 223 mm, slice thickness 8 mm, and gap: 0.7 mm. Sequences: breath-hold axial TSE T2-weighted imaging (TR/TE: 368/80 ms), breath-hold coronal single-shot T2-weighted imaging (TR/TE: 704/310 ms), in-phase axial GRE T1-weighted (TR/TE: 10/4.5 ms), out-of-phase axial GRE T1-weighted (TR/TE:10/2.2 ms), and respiratory-triggered axial DWI (echo-planar imaging; *b*-values, 0 and 800 s/mm^2; TR/TE: 3062/62 ms). Post-contrast T1 fat-saturated THRIVE imaging was performed (late arterial 20-30 s; portal venous 60-90 s; and delayed 180-210 s) after injection of 0.1 mmol/kg gadolinium contrast media (TR/TE: 4/1.5 ms), flip angle 10^0, and slice thickness 2-3 mm.

Imaging analysis

The MRI examinations were first reviewed by a coordinator radiologist with 5 years of experience in liver imaging, who revealed 69 hepatic observations in 49 patients, for which a map was generated to allocate the segmental location of the observation, and then he assigned an ordinal number to each MRI series. The image series were independently interpreted by 2 radiologists with 4 and 3 years of experience in liver imaging, respectively, using a secondary workstation (Phillips Advantage Windows workstation). Each hepatic observation was evaluated according to the LI-RADS v.2018 lexicon [9], which included 4 major features; non-rim arterial hyperenhancement (APHE), non-peripheral washout appearance (washout), enhancing capsule, lesion size, and threshold growth, which could not be evaluated because this study prospectively evaluated retrospective data and it included only 1 MRI examination for each patient. The optional ancillary features are a diverse group including those that favour HCC as mosaic architecture, fat in mass, blood products in mass, or nodule-in-nodule architecture, those that favour malignancy in general as mild to moderate T2 hyperintensity and diffusion restriction, and those that favour benignity as marked T2 hyperintensity, iron in mass, and undistorted vessels. The observation was categorized as LR-1 for definitely benign (Figure 1), LR-2 for the probably benign (Figure 2), LR-3 for the intermediate probability of HCC (Figure 3), LR-4 for probably HCC (Figure 4), LR-5 for definitely HCC (Figure 5), LR-TIV (tumour in vein) for enhancing soft tissue in vein, with or without parenchymal mass (Figure 6), and LR-M for targetoid or non-targetoid mass lesion with radiological features suggesting non-HCC malignancy (Figure 7).

Statistical analysis

Data were analysed using Statistical Package for Social Science (IBM SPSS statistics for windows, V. 22.0. Armonk, NY. USA). The qualitative data were described as number and per cent. To test the inter-reader agreement, Cohen's kappa coefficient (κ) test was performed for categorical and ordinal variables using cross-tabulation, and the interclass correlation (ICC) test was performed for the continuous variables. The 95% confidence interval was calculated. The κ and ICC tests were statistically significant as $p < 0.05$. Kappa agreement and ICC were interpreted as 0.01-0.20: slight agreement, 0.21-0.40: fair agreement, 0.41-0.60: moderate agreement, 0.61-0.80: substantial agreement, and 0.81-0.99: almost perfect agreement.

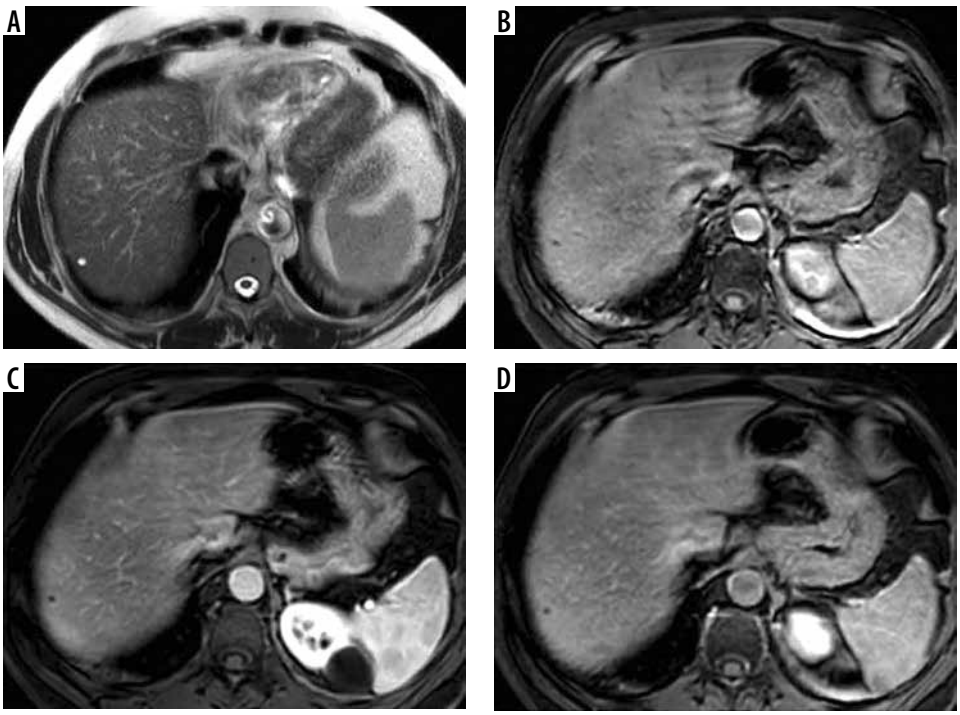

Figure 1. LR-1. Hepatic cyst. **A)** Axial T2-weighted image shows a high signal subcapsular hepatic lesion. **B-D)** No enhancement was seen in the arterial **(B)**, portal venous **(C)**, or delayed **(D)** phases

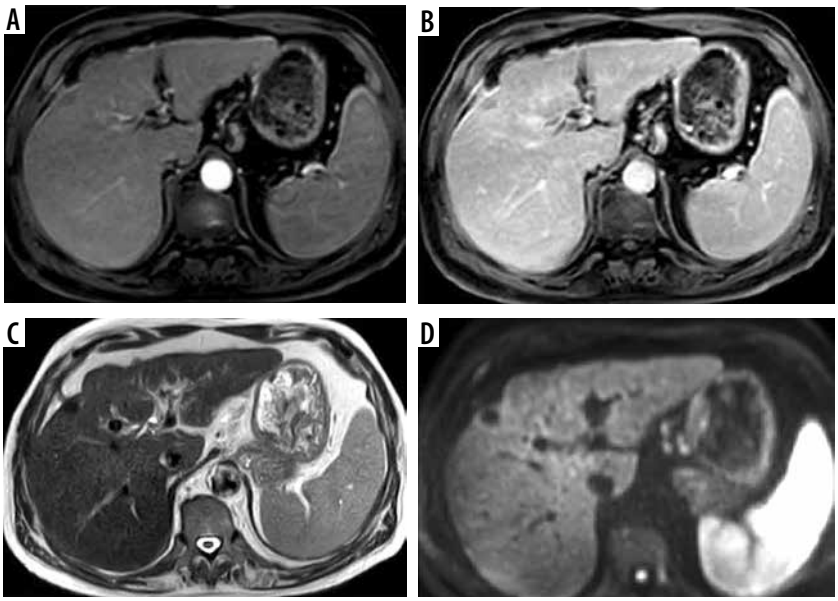

Figure 2. LR-2. Regenerative siderotic nodule in cirrhotic liver. **A)** Arterial phase shows a subcapsular hepatic focal lesion with no arterial hyperenhancement. **B)** Portal venous phase shows no washout or enhancing capsule. **C)** T2-weighted image shows a low signal hepatic lesion. **D)** Diffusion-weighted imaging shows no diffusion restriction in the hepatic lesion

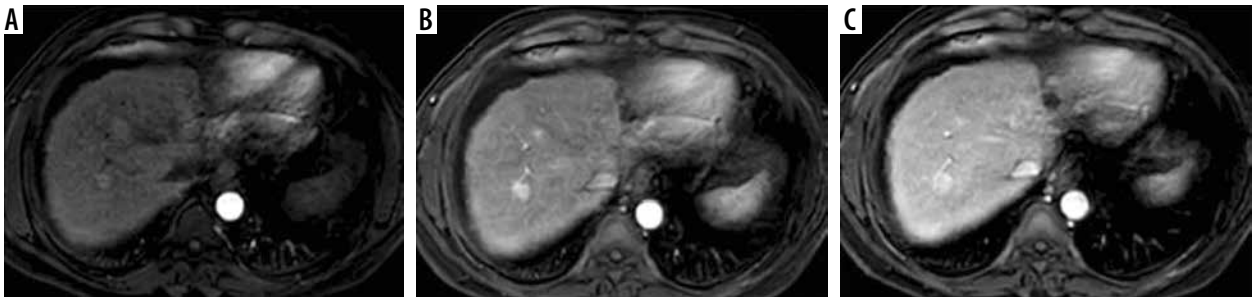

Figure 3. LR-3. **A)** Arterial phase image shows 2 hepatic focal lesions measuring about 1 cm with arterial hyperenhancement. **B, C)** Portal venous **(B)** and delayed **(C)** phases show no evidence of washout

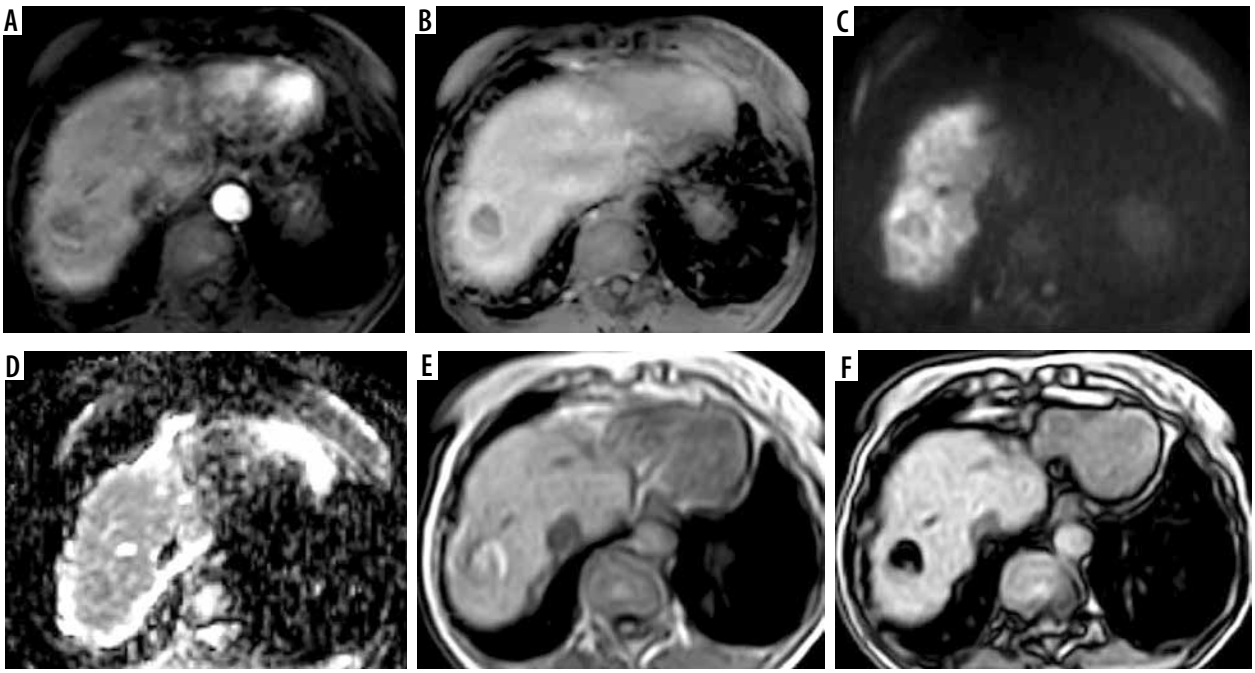

Figure 4. LR-4. **A)** Arterial phase image shows hepatic focal lesion at sub-segment VIII with arterial hyperenhancement. **B)** Delayed phase shows no evidence of washout with enhancing capsule. **C, D)** Diffusion-weighted imaging **(C)** and ADC **(D)** show no diffusion restriction. **E, F)** T2-weighted image **(E)** shows bright signal fat that shows loss of signal in the out of phase image **(F)**

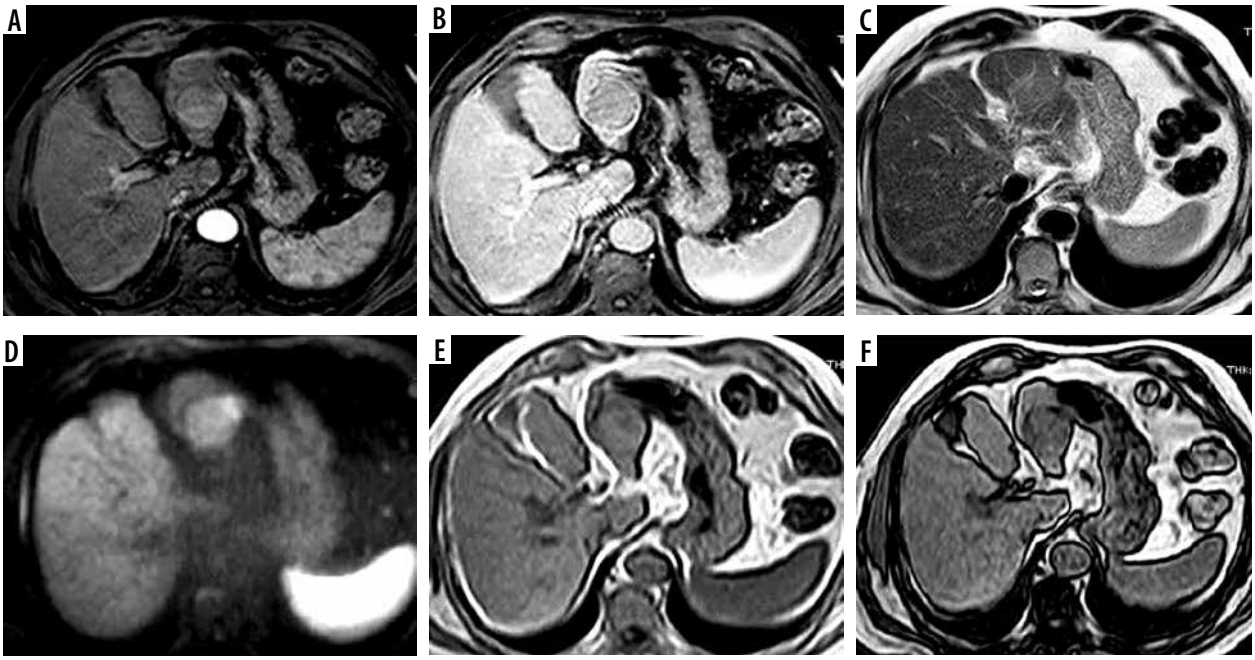

Figure 5. LR-5. **A)** Arterial phase shows a hepatic lesion in the left hepatic lobe with arterial hyperenhancement. **B)** The delayed phase shows washout with enhancing capsule. **C)** T2-weighted image shows an intermediate T2 signal. **D**) Diffusion-weighted imaging shows focal diffusion restriction. **E, F)** Foci of bright signal fat are seen in T1-weighted image **(E)** showing loss of signal in the out-of-phase image **(F)**

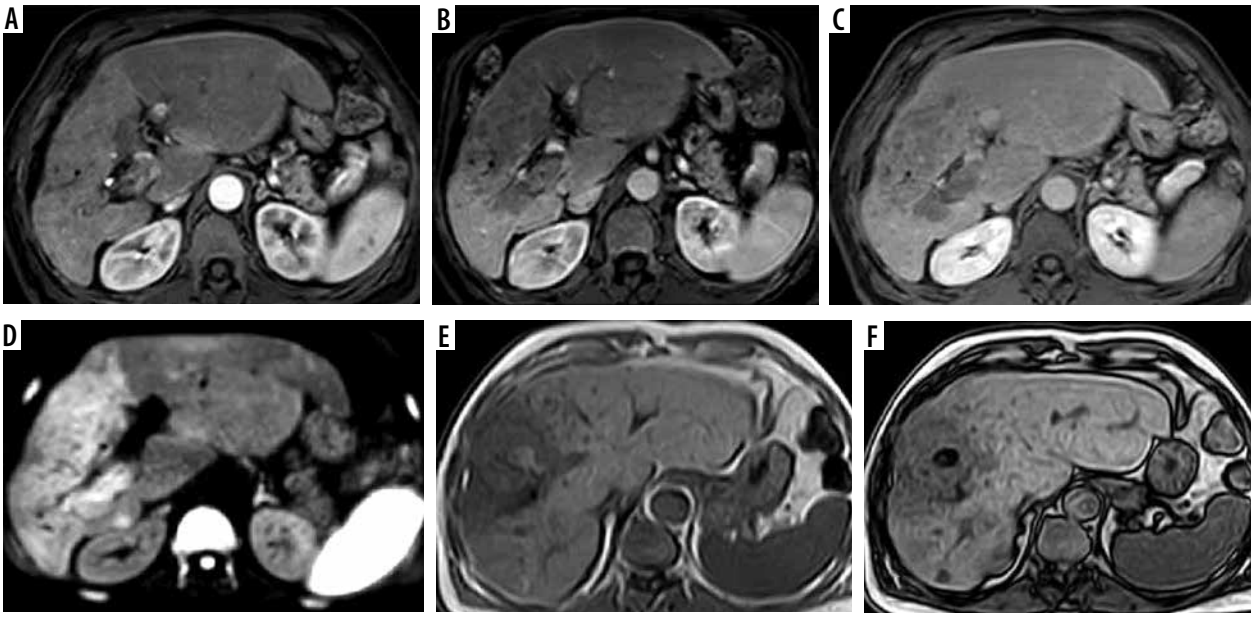

Figure 6. LR-TIV. **A)** Arterial phase image shows an infiltrative lesion with tumoral vein thrombosis in the right portal vein with arterial hyperenhancement. **B, C)** Portal venous **(B)** and delayed **(C)** phases show washout. **D)** Diffusion-weighted imaging shows diffusion restriction. **E, F)** Foci of bright signal are seen in axial T1-weighted image **(E)** showing loss of signal in out-of-phase images **(F)** denoting fat content

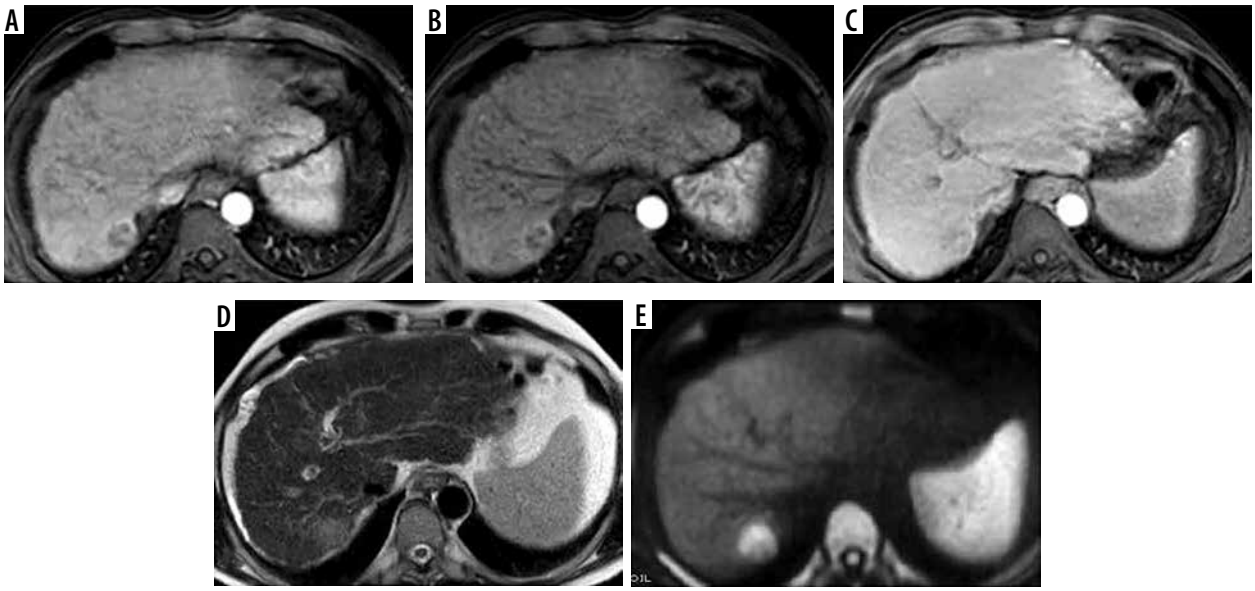

Figure 7. LR-M. **A)** Arterial phase image shows a hepatic focal lesion with rim arterial hyperenhancement and an enhancing centre. **B)** The portal venous phase shows no evidence of washout. **C)** The delayed phase shows no washout of the central enhancing area. **D)** T2-weighted image shows an intermediate T2 signal. **E)** Diffusion-weighted imaging shows diffusion restriction

Results

Forty-nine patients with 69 hepatic observations were examined, 35 (71.5%) and 14 (28.5%) cases were male and female, respectively, and the mean patient age was 60.39 ± 12.42 years (range 29 to 82 years).

A substantial agreement was noted for APHE with $\kappa = 0.796$ (95% CI: 0.653-0.939; $p < 0.001$) and 89.9% agreement. The washout and the enhancing capsule also showed a substantial agreement with $\kappa = 0.799$ and 0.772, respectively (95% CI: 0.624-0.933 and 0.615-0.928, respectively; $p < 0.001$), and agreement of 89.8% (Table 1).

In terms of ancillary features that favour HCC, there was almost perfect agreement for mosaic architecture, fat in mass, blood products in mass, and nodule-in-nodule architecture, with a κ from 0.818 to 1 ($p < 0.001$) (Table 2). A substantial agreement was noted for the ancillary features favouring malignancy in general, with $\kappa = 0.754$ and 0.718 ($p < 0.001$) for mild to moderate T2 hyperintensity and restricted diffusion, respectively (Table 3).

As regards the ancillary features favouring benignity, an almost perfect agreement was noted for marked T2 hyperintensity and iron in mass with $\kappa = 1$ ($p < 0.001$), but substantial agreement was found between the 2 read-

ers for undistorted vessels, with κ = 0.766 ($p < 0.001$) (Table 4).

The Cohen's κ coefficient showed a substantial agreement for the final LI-RADS category with κ = 0.651 (95% CI: 0.525-0.776; $p < 0.001$) and agreement of 70.9% (Table 5); the weighted κ showed higher yet still substantial agreement with weighted κ at 0.786 (95% CI: 0.697-0.876; $p < 0.001$). An almost perfect agreement was detected for LI-RADS TIV with κ = 0.818 (95% CI: 0.620-1; $p < 0.001$) and agreement of 95.7%.

The mean hepatic lesion diameter measured by reader (1) and (2) was 32.6 mm (± 36.2) and 33.1 mm (± 35.2),

Table 1. Inter-reader agreement of the major features

Major feature	Reader (1)	Reader (2)	Matched cases	κ	95% CI	*p*- value	Percent agreement
Aarterial hyperenhancement[a]	36	39	34	0.796	0.653-0.939	< 0.001*	89.9
Washout[b]	23	26	21	0.799	0.624-0.933	< 0.001*	89.8
Enhancing capsule	19	26	19	0.772	0.615-0.928	< 0.001*	89.8

[a]Non-rim arterial phase hyperenhancement. [b]Non-peripheral washout appearance. *Significant *p*-value

Table 2. Inter-reader agreement of ancillary features favouring hepatocellular carcinoma

Ancillary feature	Reader (1)	Reader (2)	Matched cases	κ	95% CI	*p*-value	Percent agreement
Blood products in mass	3	3	3	1	1-1	< 0.001*	100
Nodule-in-nodule	2	2	2	1	1-1	< 0.001*	100
Mosaic architecture	10	9	9	0.939	0.821-1	< 0.001*	98.5
Fat in mass	5	7	5	0.818	0.573-1	< 0.001*	97.1

*Significant *p*-value

Table 3. Inter-reader agreement of ancillary features favouring malignancy in general

Ancillary feature	Reader (1)	Reader (2)	Matched cases	κ	95% CI	*p*-value	Percent agreement
T2 hyperintensity (mild-moderate)	45	41	39	0.754	0.595-0.912	< 0.001*	88.1
Restricted diffusion	21	28	20	0.718	0.551-0.884	< 0.001*	87.0

*Significant *p*-value

Table 4. Inter-reader agreement of ancillary features favouring benignity

Ancillary feature	Reader (1)	Reader (2)	Matched cases	κ	95% CI	*p*-value	Percent agreement
Iron in mass	1	1	1	1	1-1	< 0.001*	100.0
Marked T2 hyperintensity	20	20	20	1	1-1	< 0.001*	100.0
Undistorted vessels	54	51	50	0.766	0.596-0.936	< 0.001*	91.3

*Significant *p*-value

Table 5. Inter-reader agreement of the final LI-RADS category

Major feature	Reader (1)	Reader (2)	Matched cases	κ	95% CI	*p*- value	Percent agreement
LR-1	6	8	4				
LR-2	13	14	9				
LR-3	18	14	13				
LR-4	9	2	2				
LR-5	13	16	12				
LR-TIV	8	11	8				
LR-M	2	4	1				
LI-RADS				0.651	0.525-0.776	< 0.001*	70.9

respectively, with an excellent correlation between the 2 readers as the ICC = 0.977 (CI 95%: 0.964-0.986; $p < 0.001$).

Discussion

The frequency of HCC is increasing all over the world. Viral hepatitis represents the most common aetiology of HCC [1]. Definite early diagnosis may allow curative treatment opportunities for patients. Due to biopsy-related complications, the diagnosis of HCC is strongly dependent on imaging modalities, with consequently increased radiologist responsibility for HCC diagnosis [10]. Radiological reporting standardization with a structured algorism is considered the new radiological era, which helps to give a discrete answer to the clinical question of concern with significant participation in the next step of patient management according to radiological imaging suspicion.

The LI-RADS was released by ACR in an attempt to standardize the imaging interpretation and reduce the variability among radiological diagnoses. Assessment of the inter-reader agreement has become of utmost importance in the case of HCC as the diagnosis, and hence the treatment-based decision is based on the imaging features with no need for lesion biopsy in every case [11-14].

In the current study, the inter-reader agreement of the major features, the optional ancillary features, and the overall LI-RADS category were assessed using the dynamic MRI imaging protocol and LI-RADS v2018, and it revealed substantial agreement for detection of APHE, washout, and the enhancing capsule. In APHE the hepatic lesion enhances after contrast injection more than the hepatic parenchyma, and its MRI signal become more intense. The non-rim arterial hyperenhancement is usually noted in HCC and the rim arterial hyperenhancement is usually noted in malignant lesions other than HCC as metastases and cholangiocarcinomas, so it is used as a feature for lesion assignment as the LR-M category [15]. The non-peripheral washout feature is characterized as hepatic focal lesion becoming hypo-enhancing with low signal compared with the background hepatic tissue, and it is best appreciated during the portal venous or delayed phase (extracellular phase). Peripheral washout is defined as a lesion with hypo-enhancing periphery relative to its centre and the surrounding liver parenchyma, and it is not typical for HCC or benign hepatic lesion, but it is mostly seen with other hepatic malignant lesions, particularly metastases and cholangiocarcinoma, so the peripheral washout feature assigns the hepatic lesion as LR-M [16,17]. The enhancing capsule appears as a peripheral enhancing rim with a smooth margin, which occurs due to retention of contrast material within extravascular connective tissue, so its appearance is pronounced in the portal venous or delayed phase [15,18,19].

Several previous studies have reviewed LI-RADS v2013 and v2014 using the dynamic MRI modalities. Lower reliability was recorded for the LI-RADS v2013 lexicon, the range of k coefficient for APHE, washout and capsular enhancement was 0.51 to 0.67, 0.48 to 0.69, and 0.37 to 0.59, respectively [20-22], but higher reliability was noted for the LI-RADS v2014, and the kappa coefficient range was 0.51 to 0.91, 0.45 to 0.83, and 0.36 to 0.89 for APHE, washout, and capsular enhancement, respectively [10,23-26]. Other studies have reviewed the agreement of LI-RADS v2017. The study by Kierans *et al.* [27] reported slight to fair inter-reader agreement of major LI-RADS features, their study was conducted using 1.5 and 3T MRI units, and used both the extracellular contrast agent and hepatobiliary agent. The study by Min *et al.* [28] was conducted using a 3T MRI system, and they reported almost perfect agreement for major features.

To our knowledge, 2 similar recent studies reviewed the reliability of LI-RADS v2018. Ludwig *et al.* [29] reviewed the diagnostic performance and the interobserver agreement of LI-RADS v2018 using both triphasic CT and dynamic MRI in a retrospective study performed in 2 liver transplant centres. Moderate agreement was reported for APHE and washout with a κ of 0.6 and 0.55, respectively. Abdel Razek *et al.* [30] reported an almost perfect agreement for APHE, washout, and capsular enhancement, with a κ of 0.948, 0.949, and 0.848, respectively. The standardized report must be a dynamic process, updated and refined continuously according to radiological experience, clinical consensus, and data validation [31,32].

Substantial agreement was noted for the final overall LI-RADS category. Studies by Fowler *et al.* [23] and Schellhaas *et al.* [24] also reported substantial agreement for the final LI-RADS category, with an ICC of 0.68, and κ of 0.61, but the study by Ludwig *et al.* [29] revealed moderate agreement for final LI-RADS category, with a κ of 0.5. On the other hand, Abdel Razek *et al.* [30] reported almost perfect agreement, with a κ of 0.99. The reliability of the overall LI-RADS category was less than that of the major feature lexicon; further refinement and accurate explanation of image interpretation will improve the reliability as the experience and data validation accumulate. This study also revealed that the mean difference between the 2 readers' final category was small with higher weighted κ (0.786) compared to non-weighted κ (0.651), reflecting good reproducibility of the LI-RADS lexicon.

LR-TIV was introduced into LI-RADS v2017, replacing the previous LR-5V, and it is characterized by enhancing soft tissue into vein whether a parenchymal mass was noted or not. The current study revealed an almost perfect agreement for detection of LR-TIV. Abdel Razek *et al.* [30] also reported almost perfect agreement for LR-TIV, and Ludwig *et al.* [29] revealed substantial agreement for this newly updated feature.

Although the detection rate of the ancillary features was significantly variable, this study revealed almost perfect agreement for the ancillary features favouring HCC, and substantial to almost perfect agreement for other ancillary features. Min *et al.* [28] reported substantial to al-

most perfect agreement for some of the ancillary features. The ancillary features could be used to enhance lesion characterization, increase radiologist confidence for diagnosis, or adjust the LI-RADS category by no more than 1 category, with the exception of the LR-5 category [15,18]. An abbreviated MRI protocol without administration of contrast media could be used for surveillance of high-risk patients using the ancillary features for diagnosis of hepatic malignancy and HCC, especially in patients with severe renal impairment.

The current study revealed almost perfect agreement for hepatic lesion diameter measurement; similar agreement for the diameter measurement was also noted in many studies [20-22,30]. However, Sevim *et al.* [10] revealed less agreement for diameter measurement (ICC = 0.676). The precise diameter measurement is an important step in the LI-RADS lexicon because the final LI-RADS category is dependent on the lesion size.

The structured reporting system has many advantages, providing a definite clear language between radiologists, clinician, and patients, facilitating the communication between them, and providing comprehensive and consistent reporting by defining the major and ancillary features compared to free-text non-defined reporting. To standardize imaging interpretations, ongoing education with experience accumulation and revised and more comprehensive definitions may be needed.

The limitations met in this study were as follows: first, the sample size was somewhat limited. Schellhaas *et al.* [24] conducted their study in 50 hepatic lesions, but the current study included 69 hepatic lesions. Second, the inter-reader agreement of threshold growth was not determined. Third, the inter-reader agreement of the LI-RADS lexicon after HCC locoregional management was missed in this study, so a further study evaluating the LI-RADS treatment response with the implementation of functional imaging may be of value. Lastly, inter-modality agreement between computed tomography and MRI was not performed in our study.

Conclusions

The LI-RADS major features of APHE, washout, and enhancing capsule had significant inter-reader agreement; moreover, the ancillary features suggesting hepatocellular carcinoma, malignancy in general, and benignity had substantial to near-perfect inter-reader agreement.

Conflict of interest

The authors report no conflict of interest.

References

1. Mittal S, El-Serag HB. Epidemiology of hepatocellular carcinoma: consider the population. J Clin Gastroenterol 2013; 47S: S2-S6.
2. Bray F, Ferlay J, Soerjomataram I, et al. Global cancer statistics 2018: GLOBOCAN estimates of incidence and mortality worldwide for 36 cancers in 185 countries. CA Cancer J Clin 2018; 68: 394-424.
3. London WT, Petrick JL, McGlynn KA. Liver cancer. In: Thun MJ, Linet MS, Cerhan JR, Haiman CA, Schottenfeld D (eds.). Cancer Epidemiology and Prevention. 4th ed. New York: Oxford University; 2018. pp. 635-660.
4. Kokudo N, Hasegawa K, Akahane M, et al. Evidence-based clinical practice guidelines for hepatocellular carcinoma: the Japan Society of Hepatology 2013 update (3rd JSH-HCC Guidelines). Hepatol Res 2015; 45: 23-127.
5. Azab EA, Abdelrahman AS, Ibrahim MEA. A practical trial to use Thyroid Imaging Reporting and Data System (TI-RADS) in differentiation between benign and malignant thyroid nodules. Egypt J Radiol Nucl Med 2019; 50: 17.
6. Mitchell DG, Bruix J, Sherman M, Sirlin CB. LI-RADS (Liver Imaging Reporting and Data System): summary, discussion, and consensus of the LI-RADS Management Working Group and future directions. Hepatology 2015; 61: 1056-1065.
7. Elsayes KM, Kielar AZ, Agrons MM, et al. Liver Imaging Reporting and Data System: an expert consensus statement. J Hepatocell Carcinoma 2017; 4: 29-39.
8. Elsayes KM, Hooker JC, Agrons MM, et al. 2017 version of LI-RADS for CT and MR imaging: an update. Radiographics 2017; 37: 1994-2017.
9. Elsayes KM, Kielar AZ, Elmohr MM, et al. White paper of the Society of Abdominal Radiology hepatocellular carcinoma diagnosis disease-focused panel on LI-RADS v2018 for CT and MRI. Abdom Radiol 2018; 43: 2625-2642.
10. Sevim S, Dicle O, Gezer NS, et al. How high is the inter-observer reproducibility in the LIRADS reporting system? Pol J Radiol 2019; 84: 464-469.
11. Willatt JM, Hussain HK, Adusumilli S, Marrero JA. MR imaging of hepatocellular carcinoma in the cirrhotic liver: challenges and controversies. Radiology 2008; 247: 311-330.
12. Pomfret EA, Washburn K, Wald C, et al. Report of a national conference on liver allocation in patients with hepatocellular carcinoma in the United States. Liver Transpl 2010; 16: 262-278.
13. Bruix J, Sherman M; American Association for the Study of Liver Diseases. Management of hepatocellular carcinoma: an update. Hepatology 2011; 53: 1020-1022.
14. Wald C, Russo MW, Heimbach JK, et al. New OPTN/UNOS policy for liver transplant allocation: standardization of liver imaging, diagnosis, classification, and reporting of hepatocellular carcinoma. Radiology 2013; 266: 376-382.
15. Kielar AZ, Elsayes KM, Chernyak V, et al. LI-RADS version 2018: what is new and what does this mean to my radiology reports? Abdom Radiol 2019; 44: 41-42.
16. Choi JY, Lee JM, Sirlin CB. CT and MR imaging diagnosis and staging of hepatocellular carcinoma. II. Extracellular agents, hepatobiliary agents, and ancillary imaging features. Radiology 2014; 273: 30-50.

17. Mamone G, Miraglia R. The "peripheral wash-out sign" in hepatic malignant lesions. Abdom Radiol (NY) 2019; 44: 2937-2938.
18. Cerny M, Chernyak V, Olivié D, et al. LI-RADS version 2018 ancillary features at MRI. Radiographics 2018; 38: 1973-2001.
19. van der Pol CB, Lim CS, Sirlin CB, et al. Accuracy of the Liver Imaging Reporting and Data System in computed tomography and magnetic resonance image analysis of hepatocellular carcinoma or overall malignancy – a systematic review. Gastroenterology 2019; 156: 976-986.
20. Davenport MS, Khalatbari S, Liu PS, et al. Repeatability of diagnostic features and scoring systems for hepatocellular carcinoma by using MR imaging. Radiology 2014; 272: 132-142.
21. Barth BK, Donati OF, Fischer MA, et al. Reliability, validity, and reader acceptance of LI-RADS: an in-depth analysis. Acad Radiol 2016; 23: 1145-1153.
22. Bashir MR, Huang R, Mayes N, et al. Concordance of hypervascular liver nodule characterization between the organ procurement and transplant network and liver imaging reporting and data system classifications. J Magn Reson Imaging 2015; 42: 305-314.
23. Fowler KJ, Tang A, Santillan C, et al. Interreader reliability of LI-RADS version 2014 algorithm and imaging features for diagnosis of hepatocellular carcinoma: a large international multireader study. Radiology 2018; 286: 173-185.
24. Schellhaas B, Hammon M, Strobel D, et al. Interobserver and intermodality agreement of standardized algorithms for non-invasive diagnosis of hepatocellular carcinoma in high-risk patients: CEUS-LI-RADS versus MRI-LI-RADS. Eur Radiol 2018; 28: 4254-4264.
25. Ehman EC, Behr SC, Umetsu SE, et al. Rate of observation and inter-observer agreement for LI-RADS major features at CT and MRI in 184 pathology proven hepatocellular carcinomas. Abdom Radiol (NY) 2016; 41: 963-969.
26. Ehman EC, Behr SC, Umetsu SE, et al. Increased interreader agreement in diagnosis of hepatocellular carcinoma using an adapted LI-RADS algorithm. Eur J Radiol 2017; 86: 33-40.
27. Kierans AS, Makkar J, Guniganti P, et al. Validation of Liver Imaging Reporting and Data System 2017 (LI-RADS) criteria for imaging diagnosis of hepatocellular carcinoma. J Magn Reson Imaging 2019; 49: 205-215.
28. Min JH, Kim JM, Kim YK, et al. Prospective intraindividual comparison of magnetic resonance imaging with gadoxetic acid and extracellular contrast for diagnosis of hepatocellular carcinomas using the Liver Imaging Reporting and Data System. Hepatology 2018; 68: 2254-2266.
29. Ludwig DR, Fraum TJ, Cannella R, et al. Hepatocellular carcinoma (HCC) versus non-HCC: accuracy and reliability of Liver Imaging Reporting and Data System v2018. Abdom Radiol (NY) 2019; 44: 2116-2132.
30. Abdel Razek AAK, El-Serougy LG, Saleh GA, et al. Interobserver agreement of magnetic resonance imaging of liver imaging reporting and data system version 2018. J Comput Assist Tomogr 2020; 44: 118-123.
31. Abdelaziz TT, Abdel Razk AAK, Ashour MMM, Abdelrahman AS. Interreader reproducibility of the Neck Imaging Reporting and Data system (NI-RADS) lexicon for the detection of residual/recurrent disease in treated head and neck squamous cell carcinoma (HNSCC). Cancer Imaging 2020; 20: 61.
32. Abdelrahman AS, Ashour MMM, Abdelaziz TT. Predictive value of neck imaging reporting and data system (NIRADS) in CECT/CEMRI of laryngeal and oral cavity squamous cell carcinoma. Egypt J Radiol Nucl Med 2020; 51: 241.